

Visualization of Connectivity in Octree Based Models

Leon L. Fedenczuk and Brian Wyvill

May 13, 1994

Department of Computer Science, University of Calgary
2500 University Dr. NW, Calgary T2N 1N4 Canada

1 Abstract

An interesting problem in the oil and gas industry is the visualization of the movement of oil and gas in porous media. In our work we have simulated the porous media using a pointer-based octree, representing the distribution of pores and grains. This data structure allows us to model the connectivity of the pores and thus visualize fluid penetration within the media. Whereas earlier models represent a serious simplifications or two dimensional homogeneous layers, our model provides us with a statistically accurate distribution in three dimensions and thus a more accurate representation of the connectivity.

In this paper we present our data structure and the techniques which were used to create models of porous media and their porous networks. Next, we present algorithms for connectivity in octrees and we show how to apply them to modelling and visualization of fluid penetration in porous media.

2 Introduction

2.1 Problem definition

Reservoir performance can be predicted from rock modelling and simulation techniques. The quality of such processes is directly dependent on the quality of the numerical model and the numerical description of the existing information. The most important factors is the quality of the description for porosity, permeability and fluid distributions (see [Fedenczuk 92]) and their realizations.

Computer modelling of porous media can be advanced through a combination of solid modelling, visualization, stochastic description, numerical analysis, and analysis of connectivity in the octree based models (see [Samet 90]). Connectivity is an important aspect of porous rock structure that influences the flow of fluids through rocks during production of oil or natural gas [Morrow 90]. Connectivity of real rocks has been studied by experiments with pore casts. The pore cast is made of plastic resin, which is injected into the pore system of a rock sample. After the resin hardens, the rock is then dissolved in acid, leaving a plastic replica of the rock's pore network. However, this is long and destructive type of analysis. Sequential changes can only be tested using different rock samples, which can vary significantly due to the high natural variability.

Other techniques for examining pore connectivity are based on microscopic images of the pores in 2D thin-sections of the rock [Dullien 91]. The thin-sections are analyzed to estimate pore shapes and their size distribution, from which pore connectivity and various properties are inferred. Their limitations come from the inference of the 3D properties from 2D images. Recently, we observe appearance of new techniques. They include X-ray CAT scan and NMR imaging [Kantzas 92]. The first one is based on observing the images, which intensity are derived from the attenuation of X-rays in rocks. The second allows to visualize fluid saturated 3D pore structures. This is due to the physical principles this method is based on, which observe hydrogen atomic nuclei in water.

Although actual rock samples can be tested by pushing fluids through under pressure and measuring output volumes, such test do not reveal the structure and connectivity of the pores. Taking pore casts does reveal the structure but destroys the original sample, preventing further analysis. The direct techniques (CAT scan and NMR) are expensive, provide only for the limited changes in the experimental conditions, and it is difficult to perform such test in a fashion that leaves the rock ready for further testing.

Computer modelling is an attractive technique that provides for the non-destructive simulation of porous rocks. The techniques described in this paper provide a statistically accurate simulation of the rock pore network and allow us to produce visualizations of fluid flow as well as other properties that are useful for prediction of reservoir behaviour. The visualizations (see Plates: 1-4) show the rock samples in 3D or as a series of 2D cross sections, or a pore network as an arbitrarily coloured cast, or as a model with the impregnated pore system. A more powerful effect can be achieved by the visualization of the pore network or fluid paths formed in this network through a translucent model. (see Plates 3 and 4)

2.2 Previous work

Numerical modelling of reservoir rocks and their properties such as porosity, permeability, electrical conductivity, etc., are routinely applied in petrophysics [Schwartz 87]. The approaches are simplistic as there is a limit to the size of the system of equations which can be solved using current computer technology.

The sparse data is commonly enlarged through the use of interpolation or extrapolation techniques while assuming spatial continuity [Naylor 66]. Often, stochastic approaches are used to model each parameter separately [Dimitrakop 91]. Many geometrical approximations have been applied to modelling porous structures. Some have been based on a simple pack of pipes [Edwards 91], or more complicated network of pipes connecting a set of large cubes [Spearing 91], or packs of spheres having repetitive patterns, or fractal based recursive patterns [Adler 87] and [Jacquin 87]. Other methods substitute the real medium with an electrical circuit made of a network of resistors [Fatt 56]. Such approaches, unless they are based on recursive or repetitive patterns, are algorithmically difficult and limit the amount of elements, which can be used in the modelling. On the other hand, the recursive and repetitive patterns represent gross approximations and cannot be used indiscriminately. In consequence, these models in many cases provide poor estimates and are limited in application to a particular rock type. In most cases these models are used to represent a perfect medium. An example of the perfect rock is Fontainebleau sandstone made of spherical quartz grains (known also to rock climbers!) However, this rock type is not an oil or gas bearing rock and due to its regularity is therefore easy to simulate (see [Bryant 93]).

One of the most significant achievements in the connectivity in rocks, the network approach gained momentum with the introduction of the percolation theory, which deals with random

mazes and fluid spreading phenomena [Yanuka 92]. The connecting concept was linked to the idea of pore throat and pore body by Wardlaw in [Wardlaw 78]. The pore space is considered to be a medium composed of pores relatively large empty spaces and much smaller conducting channels, called pore throats. Some of the pore throats permit flow through them and others do not. Their spatial distribution relative to the pore system controls the flow properties of the sample. This model is attractive from the point of view of describing the capillary phenomena in porous media [Macdonald 86].

2.3 The Stochastic Octree Approach

Our method for modelling, simulation, and visualization the three dimensional structure of porous media is based on a stochastic octree data structure. Unlike traditional porous rock modelling techniques, a three dimensional model is created directly, rather than from a series of two dimensional slices [Wallin 91] or packs [Visser 72] of primitives, which approximate model or pore space. The model is described stochastically using 3D distributions of basic logical primitives encoded in the octree data structure. These primitives are: pore body, pore throat, and grain body. They are built using just one geometrical primitive, a cube of variable size. The pore network is the end result of the stochastic reconstruction of the media, for which the three size distributions corresponding to pores, pore throats, and grains are taken from known samples.

3 Model Definition

A model of a pore network in three dimensions can be generated by randomly placing both pore bodies and pore throats in space, where their size could be taken from some distribution functions. The difficulties arise in modelling these primitives so that we can easily locate and link them into a pore network. This includes both the geometrical link as described above and a logical link with a computer data structure.

These two conditions have been achieved in our approach. We assume that model space can be described by distributions of:

- pore body size (empty spaces)
- pore throat size (narrow empty channels connecting pores)
- grain size (solid subvolumes)

The octree provides us with a unified and simple approach to porous media modelling. The modelling procedure treats both the pore and the pore throat as primitives built out of the same basic units (cubes) but of different sizes. The model of the network of pores and throats is built of empty cubic elements where the throats are built of the smallest size cubes. The same approach is applied to modelling grains or the rock matrix (everything that is not empty space).

In many geological rocks grain and pore size are more or less lognormally distributed. A normal distribution of the grain and pore sizes may be obtained by taking the log of the values of the pore and grain sizes. A lognormal distribution is commonly used to describe random processes that represent the product or combined effect of several lesser independent events [Ripley 88]. In modelling we wish to generate random numbers whose distribution are other than uniform. This is done by generating uniformly distributed pseudorandom numbers and using these to draw random samples from theoretical or observed frequency distributions.

The octree as a hierarchical tree structure contains leaf nodes (cubes) of exponentially decreasing size giving a simple relationship to observed distributions. Each node in the tree represents a region of the modeled rock. If the node completely describes the homogeneous region of the rock (grain/pore), it is a leaf node (black/white). If not, the node is subdivided (grey) and points to the eight children that represent the eight octants or subregions of the parent node. The stochastic process assigns to each octant a value, drawn independently at random with a probability given by grain, pore, and pore throat size distributions. Pores and pore throats are not distinguished in this process and they are drawn from the same distribution as primitives representing the same part of the media (empty space). This requires a creation of a combined distribution for pores and pore throats.

3.1 Creating the Octree

An initial cube is recursively subdivided into grey nodes along three planes (xy, xz, yz) until we reach the level in the octree where the size of the leaf nodes corresponds to the largest pore or grain. At this point some of the octants will become leaf nodes. The proportion of white/black octants will correspond to a percentage of the pores/grains from the rock sample with the size equivalent to that of the octant. The remaining nodes are further subdivided and the same process is repeated at lower levels. This provides us with a model of the porous rock, which has the same total porosity, pore and grain size distributions as the media we are simulating. A more detailed description can be found in [Fedenczuk 92].

3.2 Model Verification

The accuracy of this process is measured by comparing the input data (distributions) with statistics obtained from the computer model. These statistics are based on the count of the leaf nodes at every level of the octree. The resulting grain and pore size distributions together with volume calculations are performed from the size of the octant's edge. Preliminary results of this verification are found in [Fedenczuk 92].

4 Visualizing the Model

The visualization can include pores only, grains only, both with or without a fluid in 2D or 3D space. The 2D images (cross-sections which are slices through the three-dimensional model) allow a sequential visualization of the changes in the pore network topology along a selected direction. The 3D images correspond to the images from the classical microscopes or from the electron scanning microscope. The 2D slices correspond to the thin sections.

In every case, a rock material is displayed using a "grey" colour, which is made of red, green, and blue in equal amounts of intensity (0.70). When visualizing grains only the pore spaces are not processed leaving empty spaces. In a case when a pore topology is what we want to model the pores are displayed in a red "cast" of pore spaces. A combined visualization of rock/grain and pore systems has been used mainly in order to present the spatial relationships and for monitoring the fluid penetration.

The rendering is performed on polygonized voxels, produced by our model. Attributes such as diffuse light coefficient, reflection, and refraction when required, are assigned according to the visual requirements of the user. Pores, grains and pore throats can each be assigned different attribute sets for rendering. Plate 1 shows the model without Phong shading with four different pore and grain distributions (only solid parts). Cross sections of the selected models

are presented in Plate 2. Plate 3 and 4 show four Phong shaded views of the rock samples. Phong shading is applied for obtaining better visual effects without the artifacts associated with the cube based models. Phong shading exaggerates the solid appearance of the voxels, whilst effectively blending neighbouring voxels.

5 Simulating Fluid Penetration

Finding the connectivity of the pore network in rock samples is important, as it determines how well a pore network can conduct fluid and electrical current in petroleum reservoirs or rock samples used to estimate the reservoir properties. Analysis of flow through porous media has been under constant attention in different areas of science [Marle 81], [Hardy 90], [Ghadiri 92]. Of particular interest is the ability to distinguish area of high permeability from the non-permeable regions where fluid could not penetrate. In addition, we are interested in the behaviour of the samples as affected by changes to the porous media structure, physical conditions, and production processes.

Our algorithm does not follow the fluid as it flows in time. We are only concerned with tracing the parts of the porous network that have been penetrated by liquid and marking these nodes for visualization purposes. In this case we can start with any set of empty nodes and to each of them apply the colour of the fluid. Next, we mark the node as visited and recursively find all its empty neighbours and colour them the same way. Note that Plate 4 represents different visual realizations of the same model, solid parts (top left), a cast of empty spaces (top right), the same cast of empty spaces but this time visualized through translucent rock (bottom left) before fluid penetration. Finally, bottom right shows the same simulated rock after fluid penetration.

5.1 Visualizing Model Connectivity

Since we are simulating fluid flow, we are only interested in nodes representing empty subspaces, which can be penetrated by fluids. Fluid flow starts at an arbitrarily chosen face (we choose, the plane $x=0$) and proceeds to the opposite face (we choose our coordinate system so that the opposite face is the plane $x=1$). The first step colours all the WHITE/EMPTY nodes/octants whose faces are on the xz plane with the fluid colour (blue in the examples in this paper). At the next step each of these coloured nodes is used as the starting point for recursively finding the empty neighbours in each of the six face directions.

The algorithm implemented as function 'find_all_n' proceeds as follows:

- 1. Finds the Greater-Equal neighbour in a specific direction (the current direction).
- 2. If the neighbour is WHITE/empty and not visited yet changes it to BLUE and finds all its neighbours (recursively).
- 3. If the neighbour is GREY (subdivided) finds its smaller children, which are neighbours in the current direction (recursively).

In the following sections we describe details of the data structures and algorithms necessary to implement this process.

5.2 Connectivity in Octrees

In this section we introduce an algorithm for finding the connectivity between different nodes of the model. The algorithm proceeds by locating neighbours in a pointer-based octree which represents the model space. The method is based on techniques described by Hanan Samet [Samet 82] and [Samet 90]. However the particular requirements of our application, made it necessary to extend Samets basic neighbour finding strategy in the following manner:

- Nodes at the edge of the data structure are significant.
- Samet finds neighbours of the same or greater size, we need to also find neighbours of smaller size.

The data structure is a standard octree structure comprising of eight links between a parent and its children, and one link to the parent node. These links are used to find a nearest common ancestor, and the neighbour node in the next step.

5.3 Octant Enumeration

As mentioned above, the initial model cube placed in the origin of the XYZ coordinate system is subdivided recursively along three planes (xy, xz, yz). This results in the subdivision of the node into eight octants.

Assume that the model is viewed from a point which is located at the positive x,y, and z values. We can then split the space into left, right, down, up, back, and front orthogonal subspaces [Samet 89]. These subspaces may be allocated corresponding alpha labels: R,L,D,U,B,F are shown in figure 1. Applying appropriate symbols to all subdivisions (along xy,xz,yz planes) and at the same time applying alpha labels, we obtain a unique three character description of octants. For example the left, down, and front octant has the LDF descriptor. The numerical equivalent notation of octants are in range from 0 to 7. Similarly we treat directions in which we search for the node-octant neighbours. We annotate directions as: Left, Right, Down, Up, Back, or Front with their numerical equivalents between 0-5.

5.4 Data Structure

The octree record (structure) used in this project is in the form:

```
typedef struct _octree
{
    char code;
    int external;
    int color, depth, visited;
    struct _octree *ancestor;
    struct _octree *child[8];
}
```

The character variable code represents the type of the node and can be:

- BLACK - a leaf node representing solid/rock space
- WHITE - a leaf node representing empty space

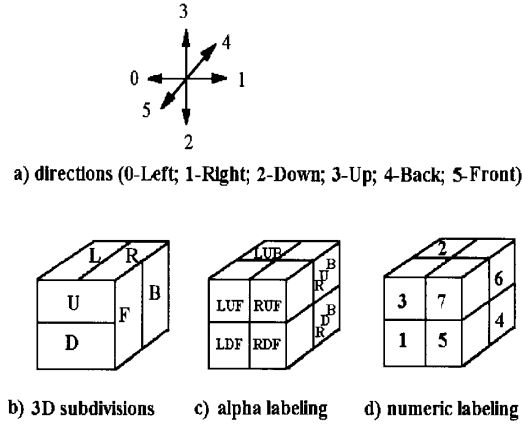


Figure 1: Direction and octant enumeration

- GREY - a subdivided node representing a mixture of solid and empty spaces.

Algorithms developed in [Samet 90] do not account for nodes on the edge face, which have no neighbours in the outside direction. The next variable 'external', in the data structure deals with this problem. The 'external' is assigned a value corresponding to the appropriate face of the root cube, which is the direction of 'outside' (if it is an internal node the value is set to -1).

Three other integer variables describe the colour, the depth, and whether a node has been already processed (visited). The last two variables in the record represent a pointer to the ancestor and an array of pointers to all eight children/octants.

5.5 Connectivity functions

These functions have been implemented based directly on the Samet's work and they return simple but important information about nodes in the model octree.

5.5.1 Samet's Primitive Connectivity Functions

The simplest functions are:

- parent() returns pointer to its parent
- child() returns pointer to a child of a specific type
- childtype() returns the type of a particular child.

These *primitive* connectivity functions are identical to those defined by Samet. More involved functions are built on these and we call them the high level connectivity functions.

Before we proceed with more functions it is necessary to point out that there are different types of neighbours: face, edge, and vertex neighbours. Presently we are concerned with face

Direction	Type			
Left	4	5	6	7
Right	0	1	2	3
Down	2	3	6	7
Up	0	1	4	5
Back	1	3	5	7
Front	0	2	4	6

Table 1: Table: SMALLER_ADJACENT

neighbours only. When simulating physical processes in porous media the other two types of neighbour connectivity make no practical sense because the edge or vertex connectivity has no real physical dimension and cannot be included in any of the flow equations. The next two functions, 'reflect' and 'adjacent', are the backbones of the algorithm for finding neighbours of equal or greater size in the octree data structure as implemented by Samet ([Samet 90]).

These functions are briefly described:

- `reflect()` returns a block/octant type of the equal size block/octant that is a neighbour in the specified direction.
- `adjacent()` returns TRUE if and only if the octant is adjacent to the face of the block in the selected direction (returns TRUE if and only if the direction is a subset of the octant enumeration e.g. `adjacent (Left, LDF)` will return TRUE because L is a subset of LDF).

5.5.2 Function for Finding Neighbours of Smaller Size

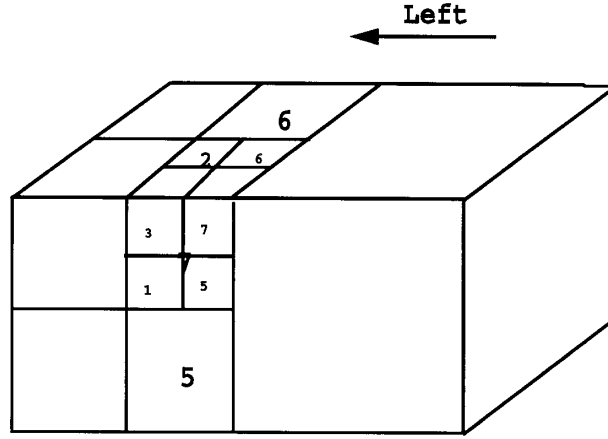
Extensions to Samet's algorithms have been built to find the connectivity to any type of neighbour, in particular to a pore/empty neighbour of smaller size. Finding smaller neighbours, is performed only if the equal size neighbour is further subdivided. Samet's algorithm is used to find a neighbour of equal or greater size.

The additional 'SMALLER_ADJACENT' table has been created (see table 1). This table gives four possible smaller neighbour types, which are a part of a grey neighbour node in the specific direction.

Figure 2 explains how the first row of this table has been created. Also the example shows that this table gives the right result independently of the level of further subdivision.

The above table is used as follows to find smaller neighbours:

- Get octant type of a possible child from SMALLER_ADJ table.
- Get octant based on the parent and octant type from above.
- If octant is WHITE/EMPTY it is marked as penetrated by fluid (BLUE) and becomes a starting point for the neighbour search ('find_all_n'), else if the octant is of the grey type the recursive process of searching for a smaller neighbour continues.



**Smaller neighbours are of type: 4,5,6,7
(1st row in SMALLER_ADJACENT_TABLE)**

Figure 2: Finding smaller neighbours

6 Results

A number of different models were used to show fluid penetration in rocks of different porosity distributions. Plate 4 shows four such samples. Initially all empty nodes had their colour assigned to red. In all cases fluid has been introduced into all empty nodes with their left planes coinciding with the xz plane. Further, nodes connected to these on the xz plane were found and their colour changed to blue as described above. The rest of the empty nodes, which were not interconnected retained their red colour. All solid nodes have been processed using the colour grey. Transparency has been used during rendering of solid parts of the model. In order to mark cells on the opposite face of the model where the process of the flow tracing stops, we changed their colour to green as shown in Plate 4.

The resulting images (Plates 3 and 4) allow visualization of a fluid invasion in porous media and location of areas where fluid could not flow. Red patches on the images clearly represent the unconnected porosity. The blue marked nodes allow one to visualize changes in connectivity as a function of changes in porosity as well as changes in pore size distribution.

6.1 Algorithm Performance

During the simulation of the fluid flow in the interconnected network of empty cells we recorded a number of nodes visited in order to find a neighbour of equal or greater size. This allows us to compare our results with the theoretical results produced by Samet [Samet 82]. The algorithm performs two major steps:

- 1. Locate the nearest common ancestor.
- 2. Retrace the path taken by using the reflect function

According to Samet the theoretical average number of nodes processed during the search for a common ancestor should approach two for octrees with a large number of subdivisions. His

theoretical average number of nodes visited during the search for neighbours of equal or greater size should be bounded by $7/2$. This means that the expected average number of nodes visited in the second part of the process (descending from the common ancestor) should not exceed two.

The statistics on effectiveness of the neighbour search corresponding to these two steps is presented in table 2.

This table provides only the statistics for the search conducted during the fluid flow through the network of pores (empty cells). Due to the process of marching through this network, some of the solid (black) nodes were not included in the process. We did not search for their neighbours.

In table 2 the model name contains a combination of two digits. The first digit represents the total number of subdivisions and the second corresponds to the level where leaf nodes start to be allocated. Each model is represented as a cube of unit size. The total number of leaf nodes and the number of empty nodes (pores) in the model are presented in the first two numerical columns of the table. The next numerical column represents the number of searches for neighbours, which is equal to the number of times the process has been performed and this is equal to the number of observation in the statistics. The average difference between the levels of the starting node and the neighbour is presented in the following column. The last five columns provide the average number of steps (nodes visited) in:

- 1. locating a common ancestor
- 2. finding a greater/equal neighbour during the reflected descent
- 3. finding a smaller neighbour (additional steps only)
- 4. finding any size neighbour (sum of the last two steps - the descent 2,3)
- 5. during the whole process of finding a neighbour.

In other words these can be described as

- 1. the number of steps up the tree,
- 2. the number of steps down the tree (GE neighbour)
- 3. additional number of steps down the tree (smaller neighbour)
- 4. sum of 2 and 3
- 5. total number of steps up and down the tree (1,2,3)

The probabilities of allocating a white/black octant (empty/solid) were kept constant at each level (below the starting level). These probabilities were assigned as 6.25% and 21.9% accordingly, with the exception of the lowest level where 50% of nodes were assigned as white and 50% of nodes were assigned as black. These percentages are typical of actual rock samples used for testing purposes.

For example in the model marked as 'r52'

- (r52) There are five levels of subdivision (starting from the root: 5,4,3,2,1,0)
- (r52) Before level 2 (levels: 5,4,3) all the nodes have been subdivided (all grey).

Model Name	# of Leaf nodes	# of empty nodes	# of searches	# of steps up	# of steps down to find GE	extra # of steps to find smaller	# of steps down to find any size	Total # of steps
r20	64	24	55	1.40	1.40	0.00	1.40	2.80
r21	29	12	43	1.35	1.19	0.09	1.28	2.63
r30	512	230	1149	1.62	1.62	0.00	1.62	3.24
r31	344	168	1090	1.63	1.47	0.06	1.53	3.16
r32	246	112	680	1.59	1.36	0.07	1.43	3.02
r40	4096	1622	7711	1.76	1.76	0.00	1.76	3.52
r41	3137	1224	6300	1.76	1.64	0.05	1.68	3.44
r42	2500	958	4180	1.72	1.53	0.07	1.60	3.32
r43	1527	616	4631	1.77	1.44	0.08	1.52	3.29
r50	32768	12747	62930	1.85	1.85	0.00	1.85	3.70
r51	24529	9332	44849	1.84	1.70	0.05	1.75	3.59
r52	18173	6940	34689	1.85	1.59	0.08	1.67	3.52
r53	11845	4507	22531	1.84	1.49	0.09	1.58	3.42
r54	7624	2884	9739	1.84	1.49	0.08	1.57	3.41
r60	262144	102040	523255	1.91	1.91	0.00	1.91	3.82
r61	198661	75588	413130	1.90	1.76	0.05	1.81	3.71
r62	143984	54653	295367	1.91	1.66	0.07	1.73	3.64
r63	99849	37847	195146	1.91	1.57	0.09	1.66	3.57
r64	76063	28717	144324	1.93	1.54	0.10	1.64	3.57
r65	33909	12776	70311	1.92	1.51	0.11	1.62	3.54
r73	836543	317860	1782721	1.95	1.61	0.09	1.70	3.65
r74	581274	220683	1163805	1.95	1.55	0.10	1.65	3.60
r75	388396	147359	749334	1.95	1.53	0.11	1.64	3.59
r76	303451	115156	643255	1.96	1.53	0.11	1.64	3.60
r76a	87704	33116	220528	1.96	1.48	0.12	1.61	3.57
r86	2088465	795120	4462631	1.98	1.54	0.11	1.65	3.63
r87	1588441	604846	3373837	1.98	1.53	0.11	1.65	3.63

Table 2: Table: Neighbour Finding Statistics

- **(6.25%)** At levels two and one (2 & 1) 6.25% of nodes have been assigned as empty (white leaf nodes)
- **(21.9%)** 21.9% of nodes have been assigned as solid (black leaf nodes). The rest have been further subdivided.
- **(50%)** At the lowest level (zero) 50% of the nodes have been assigned as empty and the other 50% as solid (no subdivision allowed).

The exception to the above rules represents model 'r76a', which had higher probabilities at each of the levels. However, the statistics for this model is not significantly different from the typical model 'r76'. The porosity of the models is calculated as the ratio of the volume of the empty nodes to the whole volume.

Figure 3 presents the average number of steps up the tree (levels traversed) in order to find a common ancestor. The experimental estimations are compared with the calculated values from Samet's formula and they are presented as a function of the number of levels in the octree. Different symbols are used to display changes due to the leaf starting level (the level at which the leaf nodes are permitted). Overall, the theoretical and experimental values follow the same trend and the differences could be due to the Samet's definition of the randomness. The differences due to the starting level are relatively low and suggest that the ancestor search is independent of this parameter.

The rest of graphs, which represent the downward movements from the ancestor already located, are significantly affected by the starting level of the leaf nodes. The first of them (Figure 4) presents the average number of steps which are required to find a neighbour of equal or greater size. The additional number of steps made during the process of finding a smaller neighbour and the sum of steps taken during a tree descent are presented in Figure 5 and Figure 6 accordingly. The average total number of nodes during the all of the stages of the neighbour search is presented in Figure 7. Overall, the number of steps during a descent and the total number of steps are effected by the starting level for the leaf nodes. The higher the starting level the smaller is the number of the steps required to find a common ancestor and the neighbour. The reverse trend is observed for the additional number of steps during the search of the smaller neighbour after the equal size neighbour is further subdivided. However, this does not affect the statistics significantly due to overall low values observed for this process. The average number of additional steps is below 0.14 mark. The total of steps exponentially grows with the number of levels and exceeds the predicted number as derived by Samet. However in Samet's case, traversals are made over all nodes including subdivided octants, whereas in our models we are only interested in finding empty neighbours of empty leaf nodes.

7 Advantages of The Stochastic Octree Technique

The methods presented provide not only display of the model externally, but also reveal the internal structure of the model during the simulation of physical processes in areas such as flowing matter, visualized boundary layers, spatial topology of the porous network, etc. For example, the proposed methodology may be used to build geometrical models of porous rocks.

The advantages of such a stochastic model, as opposed to a deterministic model, are:

- provide average behaviour
- provide for the description of local random variations

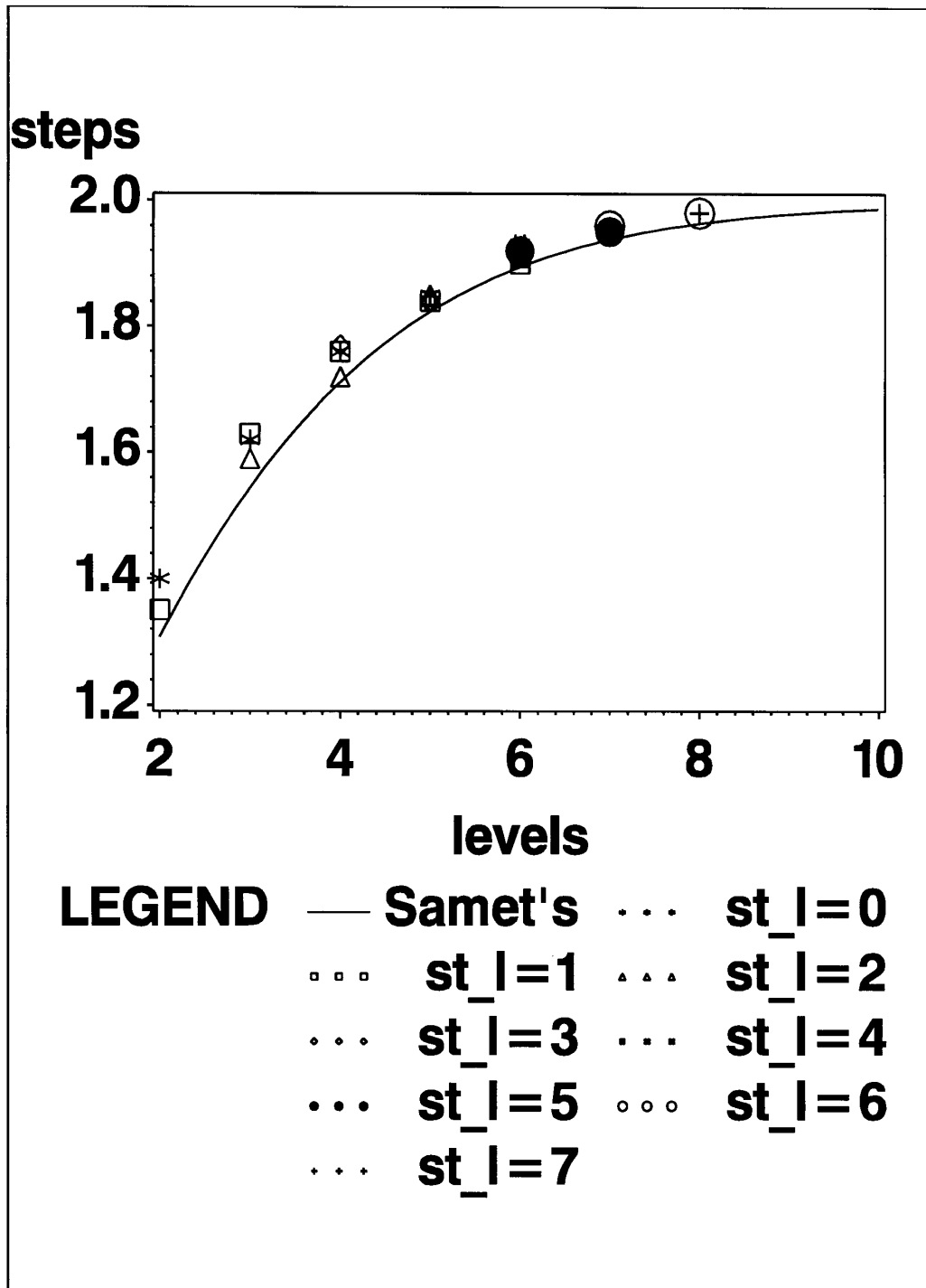


Figure 3: Number of nodes visited to find a common ancestor

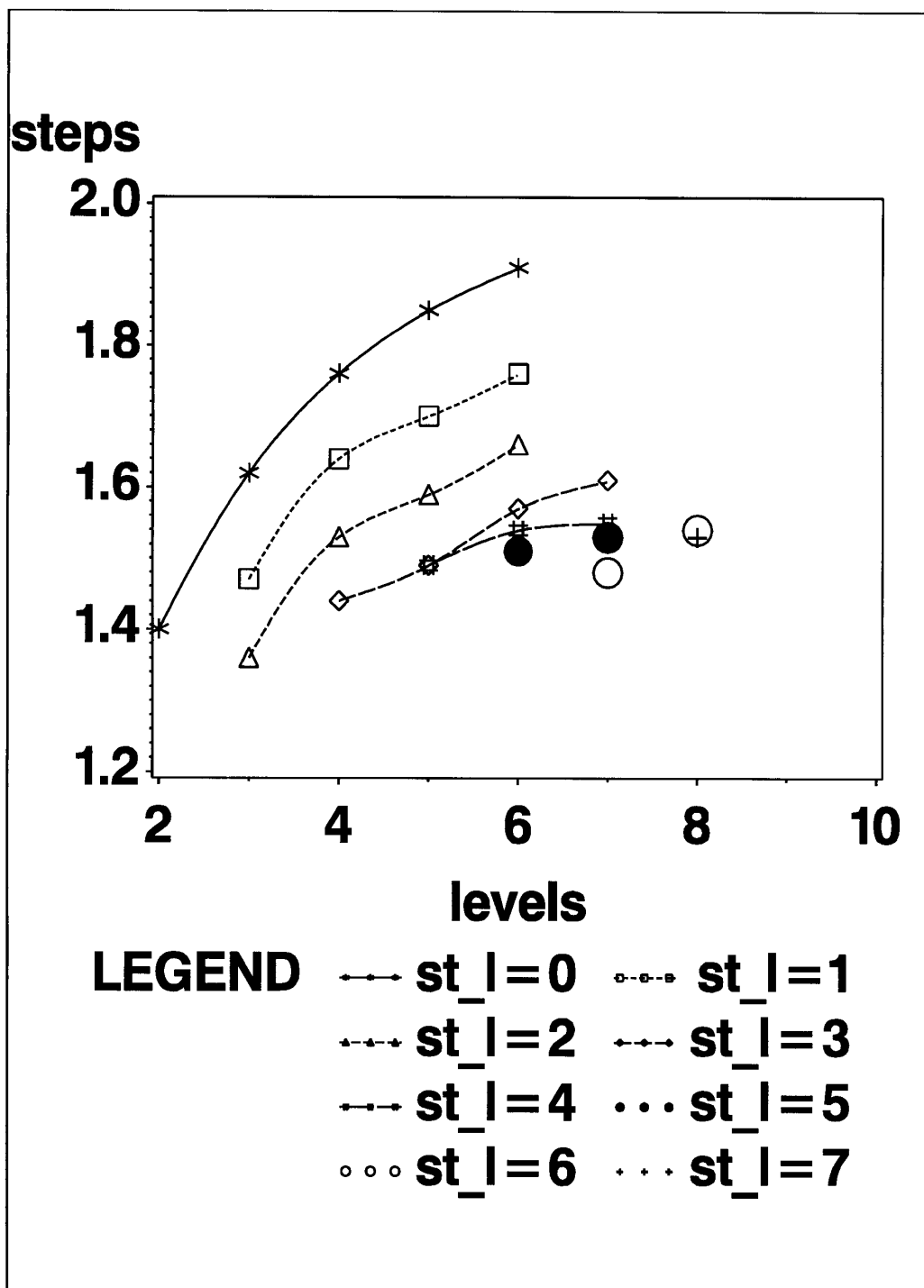


Figure 4: Number of steps down from an ancestor to find a greater or equal neighbour

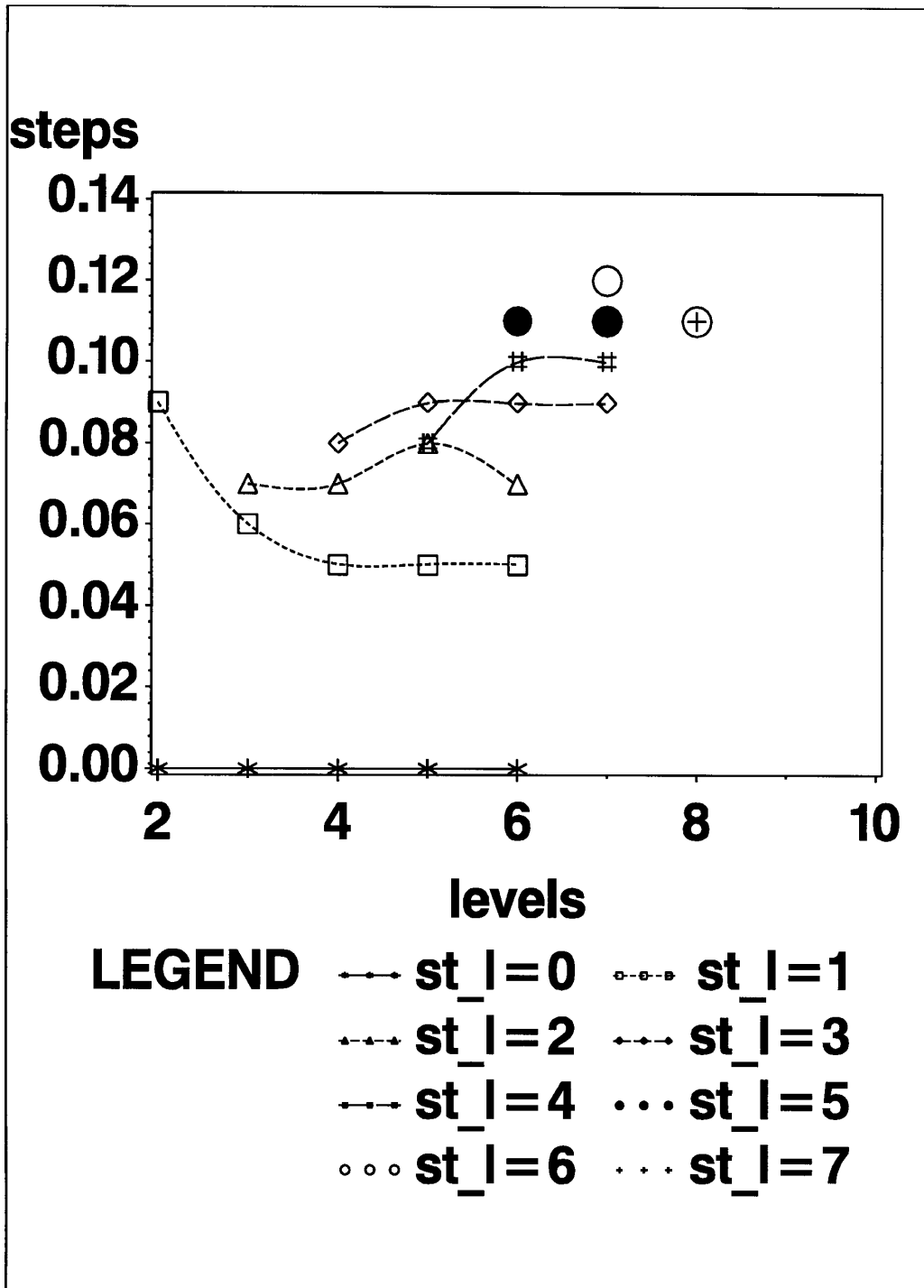


Figure 5: Number of additional steps down to find smaller neighbour

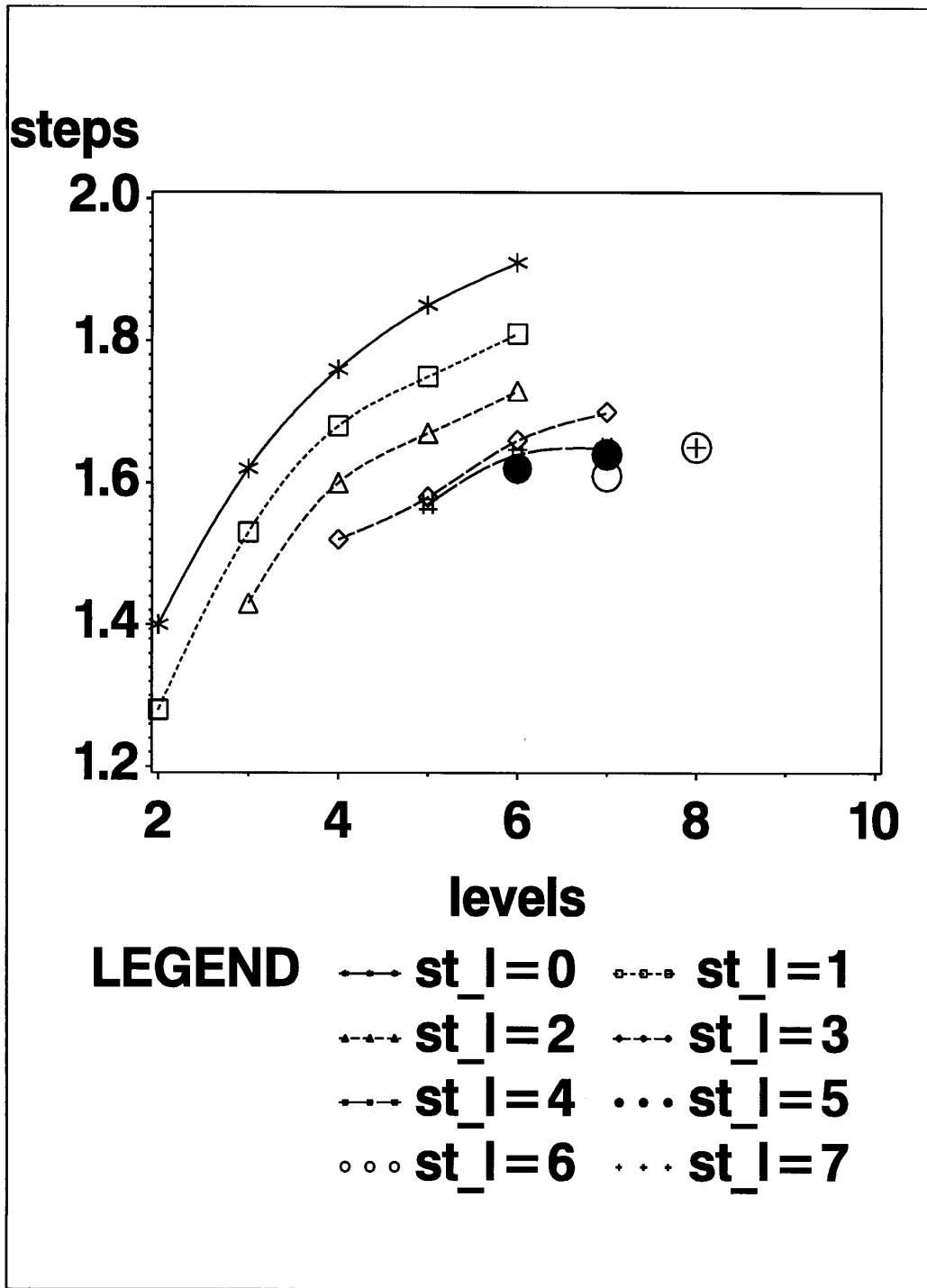


Figure 6: Number of steps down to find any type of neighbour

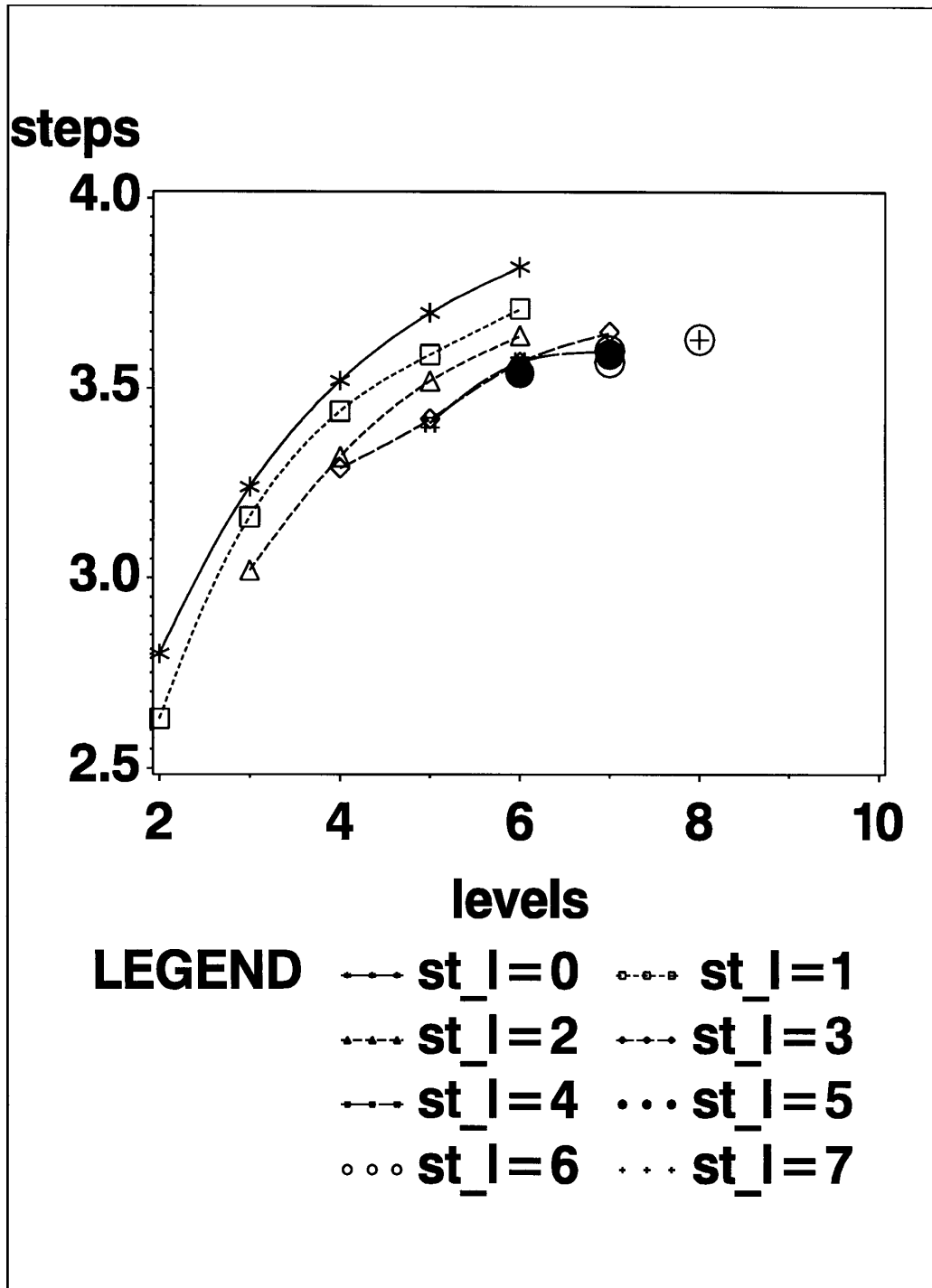


Figure 7: Total number of steps to find any type of neighbour

- enable the estimation of correlation between neighbouring locations
- provide uncertainty of the estimates
- allow the reconstruction of the media using a concise description
- finally, the stochastic description allows an effective bridge and transformation of petrophysical rock descriptions to computer data structures and numerical primitives.

Unlike traditional reservoir modelling techniques our approach allows building and visualizing models of any complexity limited only by available memory and machine cycles. Our model is sufficiently general that it can be applied to different types of fluids and minerals from which rocks are built. Our model can be easily extended to simulate such processes as a cementation, which can be defined as introducing mineral phases into a rock pore system. When cement is formed it appears as an overgrowth on the grains, and can be represented as concentric rims on the grains.

Another advantage of this technique is that we can simulate various physical properties of the porous media and provide visualizations which allow a petroleum researcher to monitor these processes. Using the various display techniques (slicing, transparency etc.) a user can visualize the rock's pore structure or spaces containing fluid in a translucent or opaque appearance.

Finally, the adaptive octree data structure represents a major improvement to a 3D array application of equal size cells by accounting for the local agglomeration and homogeneity. This lowers the requirements for the computer resources, provides much better approximation of rock structures, and facilitates the simulation of physical properties.

8 Practical Applications of The Stochastic Octree Technique

The modeling and simulation results can be used to perform:

- quick evaluation of rock parameters
- calibration of well logging tools (tools used to measure electrical and magnetic responses in oil wells).
- education
- determination of the estimation sensitivity.

Information derived from simulations will help to evaluate the potential of reservoirs and help to monitor recovery processes. If rock types in the analyzed reservoir are similar to those of the simulated sample, a user can infer all parameters without having to take long and detailed measurements or tests, thus saving time and money.

Future development may include a real time simulation system for fluid flow, simulation and interpretation of electrical and sonic properties of models as they vary with temperature, pressure, etc. The statistics associated with the estimated parameters resulting from simulations can provide the confidence intervals of the simulated values.

9 Conclusion

We have presented a method of visualizing fluid flow in porous rocks for use by petrophysicists and geophysicists interested in rock properties and reservoir simulation for testing existing hypothesis on hydrodynamic processes in rocks, changes due to natural processes, and changes due to oil and gas production in reservoir rocks. Our approach provides alternative means to investigate porous media. It allows the creation of a wide range of computer models based on the known description of naturally created rocks. Fluid behaviour in these models at different scales of complexity (geometrical and physical) can be simulated. Using this approach we can estimate and visualize other simulated physical properties (electric, sonic, etc). Finally, we can model other processes (fluid interaction, permeability, cementation, etc.) and observe the resulting changes in porous media.

To summarise:

- The models based on the octree data structure provide a powerful tool in the simulation and visualization of porous media properties.
- The average number of nodes visited during the search for the common ancestor, when searching for the neighbour of equal or greater size, increases with the number of subdivision levels in the octree. In general, this value is independent of the internal structure of the model.
- The experimental results exceed slightly the theoretical bound on average number of nodes (as a function of the number of levels) required to be visited in order to allocate the common ancestor as provided by the formula derived by Samet [Same90].
- The average number of nodes visited in the second part of the algorithm is strongly dependent on the internal structure of the model. This value decreases for models with a highly variable size of leaf nodes representing the network of empty cells.
- The total number of steps in our experiments exceed the overall upper bound of finding neighbours as cited by Samet. This is explained above.
- We expect that our research will provide the basis for a system with potential applications in petrophysics and other areas of engineering.

10 List of Plates

- Plate 1: 3D view for models with 4 different pore distributions.
- Plate 2: Cross sections of selected models.
- Plate 3: Fluid penetration in 4 different pore distributions.
- Plate 4: Fluid penetration green colour used to show the last cell of any path which ends at plane $x=1$.

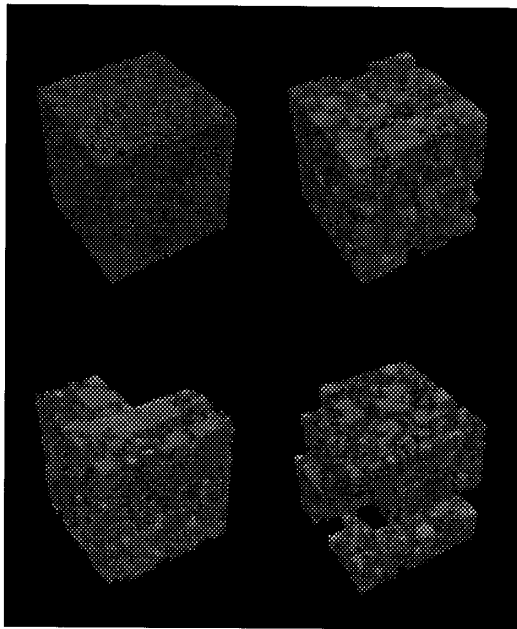


Plate 1.

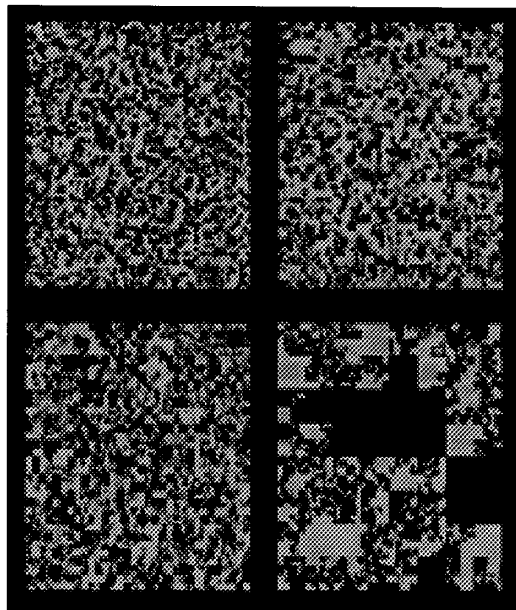


Plate 2.

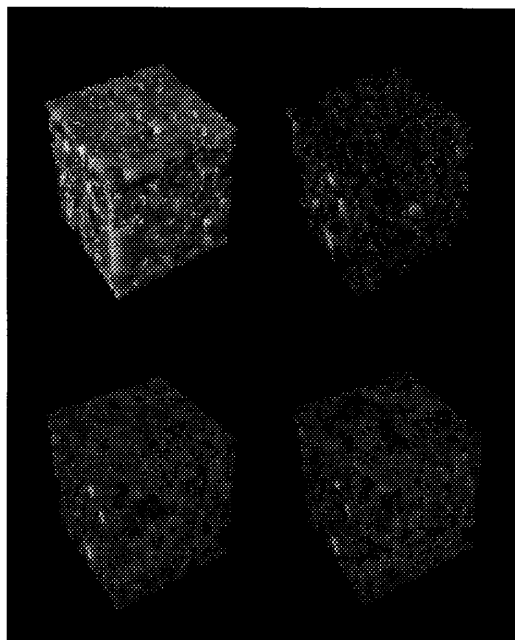


Plate 3.

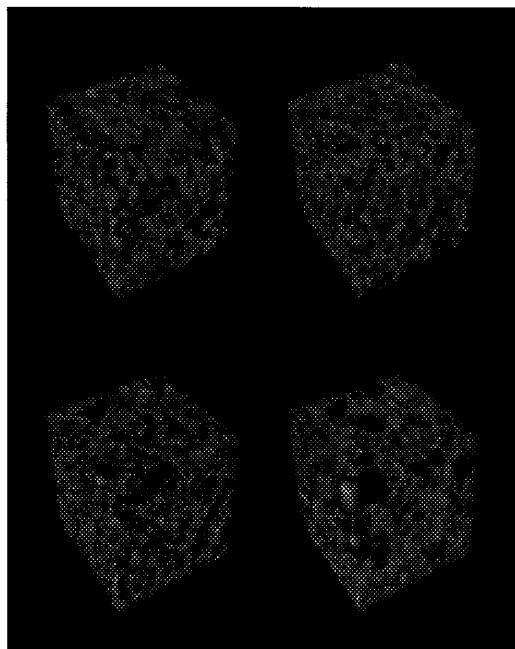


Plate 4.

References

- [Adler 87] P.M. Adler and C.G. Jacquin. Fractal Porous Media I: Longitudinal Stokes Flow in Random Carpets. *Transport in Porous Media*, 2:553–569, 1987.
- [Bryant 93] Steven Bryant, Christopher Cade, and David Mellor. Permeability Prediction from Geologic Models. *The American Association of Petroleum Geologists Bulletin*, 77(8):1338–1350, August 1993.
- [Dimitrakop 91] Roussos Dimitrakopoulos. Stochastic modelling of space dependent reservoir-rock properties. *The Journal of Canadian Petroleum Technology*, 30(4):43–51, July-August 1991.
- [Dullien 91] F.A.L. Dullien. Characterization of Porous Media - Pore Level. *Transport in Porous Media*, 6(5-6):581–606, 1991.
- [Edwards 91] D.A. Edwards, M. Shapiro, H. Brenner, and M. Shapira. Dispersion of Inert Solutes in Spatially Periodic Two-Dimensional Model Porous Media. *Transport in Porous Media*, 6(4):337–358, 1991.
- [Fatt 56] I. Fatt. The network Model of Porous Media. *Petroleum Transactions, AIME*, 1956.
- [Fedenczuk 92] Leon L. Fedenczuk and Brian Wyvill. Petrophysical Rock Modeling. *The Journal of The Canadian Well Logging Society*, 18:107–125, 1992.
- [Ghadiri 92] Hossein Ghadiri and Calvin W. Rose. *Modeling Chemical Transport in Soils*. Lewis Publishers, 2000 Corporate Blvd. N.W., Boca Raton, Florida, 1992.
- [Hardy 90] H.H. Hardy. Jots - A Mathematical Model of Microscopic Fluid Flow in Porous Media. *Transport in Porous Media*, (5), 1990.
- [Jacquin 87] C.G. Jacquin and P.M. Adler. Fractal Porous Media II: Geometry of Porous Geological Structures. *Transport in Porous Media*, 2:571–596, 1987.
- [Kantzas 92] Apostolos Kantzas, Daniel F. Marentette, and Kamal N. Jha. Computer-assisted tomography: from qualitative visualization to quantitative core analysis. *The Journal of Canadian Petroleum Technology*, 31(9):48–56, November 1992.
- [Macdonald 86] I. F. Macdonald, P. Kaufmann, and F. Dullien. Quantitative Image Analysis of Finite Porous Media. *Journal of Microscopy*, 144(3), Dec. 1986.
- [Marle 81] Charles M. Marle. *Multiphase Flow in Porous Media*. Gulf Publishing Company, Houston, Texas, 1981.
- [Morrow 90] Norman R. Morrow. *Interfacial Phenomena in Petroleum Recovery*. Marcel Dekker, Inc., 1990.
- [Naylor 66] T. H. Naylor, J.L. Balintfy, et al. *Computer Simulation Techniques*. John Wiley and Sons, 1966.
- [Ripley 88] B.D. Ripley. *Statistical Inference for Spatial Processes*. Cambridge University Press, 1988.

- [Samet 82] Hanan Samet. Neighbor Finding Techniques for Images Represented by Quadtrees. *Computer Graphics and Image Processing*, 18:37–57, 1982.
- [Samet 89] Hanan Samet. Implementing Ray Tracing with Octrees and Neighbor Finding. *Computers and Graphics*, 13(4), 1989.
- [Samet 90] Hanan Samet. *Applications of Spatial Data Structures Computer Graphics, Image Processing, and GIS*. Addison-Wesley, 1990.
- [Schwartz 87] L. M. Schwartz and S. Kimminau. Analysis of electrical conduction in the grain consolidation model. *Geophysics*, 52(10), Oct. 1987.
- [Spearing 91] Michael Spearing and G.Peter Matthews. Modelling Characteristics Properties of Sandstones. *Transport in Porous Media*, 6:71–90, 1991.
- [Visscher 72] W. M. Visscher and M. Bolsterli. Random Packing of Equal and Unequal Spheres in Two and Three Dimensions. *NATURE*, 239, Oct. 1972.
- [Wallin 91] A. Wallin. Constructing Isosurfaces from CT Data. *IEEE Computer Graphics and Applications*, 11(11), 1991.
- [Wardlaw 78] N.C. Wardlaw and J.P. Cassan. Estimation of Recovery Efficiency by Visual Observation of Pore Systems in Reservoir Rocks. *Bulletin of Canadian Petroleum Geology*, 28(4), Dec. 1978.
- [Yanuka 92] M. Yanuka. Percolation Theory Approach to Transport Phenomena in Porous Media. *Transport in Porous Media*, 7:265–282, 1992.